Correspondence

Spectral Characteristics and Motion-Compensated Restoration of Composite Frames

R. Manduchi and G. M. Cortelazzo

Abstract—**The practice of superimposing the fields of a frame is applied in various fields, for example, thermographic and biomedical imaging. The pictures obtained in this way, which are termed composite frames, are severely degraded if the scene's objects are not perfectly still. The restoration of composite frames affected by motion-induced blurring requires the ability to estimate the field displacement from composite frames. The frequency domain analysis of composite frames proposed in this work suggests a displacement estimation technique of a phase-correlation type that can be applied to composite frames.**

I. Introduction

Several imaging techniques produce their pictures by superimposing the two fields of a frame of a sequence scanned by a camera operating with an interlace ratio of 2:1. Thermograms are a typical example of this. Other equipment that is also used for computerized medical images uses the idea of superimposing the fields of a frame. In the following, we will refer to the images obtained in this way as *composite frames*.

Anybody who has ever taken a picture of a scene displayed on a television set may well have experienced a typical "staircase" effect at the edges of moving objects [1]. Such a visual effect is due to the fact that the edges of a moving object appear at close but different positions in the succeeding fields of a television sequence.

Composite frames have been developed for the recording of still scenes. If the scene taken (or the camera) is not perfectly still, as often occurs, the edge disalignment on succeeding fields becomes a rather noticeable source of visual quality degradation. Image restoration procedures for composite frames must be able to cope with this kind of motion-induced blurring.

With respect to motion effects, several techniques exist [1], [2] for restoring pictures derived from sequences supported by orthogonal (spatio-temporal) lattices [3]. The restoration of composite frames, however, must take into account the interlaced nature of the spatio-temporal lattice from which the picture is obtained. The special features of line interlacing were first recognized in p. 604 of [1].

This work examines the structure of composite frames in the frequency domain. Such an analysis is instructive as it reveals a spectral regularity that suggests the possibility of developing a phase-correlation type technique [7] for estimating the object's displacement in consecutive fields. An estimate of displacement can be used in order to realign the fields with the object's position in the first field. Such an operation may be seen as a special case of the technique commonly known as "motion-compensated deinterlacing" (see for instance [4], [5]). Unlike the algorithms commonly employed in the area of television and computer vision, the algorithm proposed is capable of measuring the displacement within one single frame (i.e., exploiting the information provided by only two succeeding fields). Thus, it can be used in cases (e.g., biomedical imagery) where only one image frame is available. As the application example shows, this simple motion deblurring method is remarkably effective.

The second section of this work analizes composite frames relative to the 2:1 interlace ratio in the frequency domain. Section III presents the displacement measurement technique and the results of its application to the motion-compensated restoration of composite frames.

Manuscript received March 9, 1993; revised October 3, 1993. This work was supported by CNR-Progetto Finalizzato Telecomunicazioni, Contract No. 91.01819.PF71. The associate editor coordinating the review of this paper and approving it for publication was Dr. M. Ibrahim Sezan.

R. Manduchi is with the Department of Electrical Engineering and Computer Science, University of California at Berkeley, Berkeley, CA 94720 USA.

G. M. Cortellazzo is with the Dipartimento di Elettronica e Informatica, Universitá di Padova, Padova, Italy.

IEEE Log Number 9406878.

II. Spectral Analysis of Composite Frames of Moving Images

A. Spectral Characteristics of Composite Frames

Consider a 2:1 interlaced scanning system: the field period T_F and the frame period T_Q (clearly $T_Q = 2T_F$). Let Δ_y be the interline distance in a frame (e.g., on the focal plane), and take the distance between two consecutive pixels of a line as Δ_x. Let $u_c(x, y, t)$ be the luminance intensity function on the focal plane (or the radiometric intensity function for thermographic systems). The sampled version of $u_c(x, y, t)$ will be denoted as $u(l\Delta_x, m\Delta_y, nT_F)$; it is only defined for values of m and n that are both even or both odd (i.e. for $(m - n) = 0 \bmod 2$).

It is well known [3] that the Fourier transform of $u(l\Delta_x, m\Delta_y, nT_F)$, which is denoted $U(k_x, k_y, f)$, is related to the Fourier transform $U_c(k_x, k_y, f)$ of $u_c(x, y, t)$ as

$$U(k_x, k_y, f) = \sum_{l,m,n=-\infty}^{\infty} U_c\left(k_x - \frac{l}{\Delta_x}, k_y - \frac{m}{2\Delta_y}, f - \frac{n}{T_Q}\right) \tag{1}$$

where sum indexes m and n are either both even or both odd.

Given integer n, signal

$$u_n(l\Delta_x, m\Delta_y) = \begin{cases} u(l\Delta_x, m\Delta_y, 2nT_F) & \text{even } m \\ u(l\Delta_x, m\Delta_y, (2n+1)T_F) & \text{odd } m \end{cases}, l, m \in Z \tag{2}$$

will be referred to as the nth *composite frame* or, in the case of thermographic imagery, as the nth *thermogram*. This section derives the Fourier transform $U_n(k_x, k_y)$ of $u_n(l\Delta_x, m\Delta_y)$ as a function of $U_c(k_x, k_y, f)$. Such a result is instrumental for the motion-compensated restoration procedure of the next section.

Let us introduce signal

$$\bar{u}(l\Delta_x, m\Delta_y, nT_Q) = u_n(l\Delta_x, m\Delta_y) \tag{3}$$

which is formed by the composite frames sequence. Signal (3) can be rewritten as

$$\bar{u}(l\Delta_x, m\Delta_y, nT_q) = u_c(l\Delta_x, m\Delta_y, 2nT_F) \cdot \frac{1 - e^{j\pi m}}{2} + u_c(l\Delta_x, m\Delta_y, (2n+1)T_F) \frac{1 + e^{j\pi m}}{2}. \tag{4}$$

The Fourier transform of (4) is

$$\begin{aligned}\bar{U}(k_x,k_y,f) &= \frac{1}{2}\sum_{l,m,n} U_c\left(k_x-\frac{l}{\Delta_x},k_y-\frac{m}{\Delta_y},f-\frac{n}{T_Q}\right)\\ &\quad-\frac{1}{2}\sum_{l,m,n} U_c\left(k_x-\frac{l}{\Delta_x},k_y-\frac{m}{\Delta_y}-\frac{1}{2\Delta_y},f-\frac{n}{T_Q}\right)\\ &\quad+\frac{1}{2}\sum_{l,m,n} U_c\left(k_x-\frac{l}{\Delta_x},k_y-\frac{m}{\Delta_y},f-\frac{n}{T_Q}\right)\\ &\quad\times e^{j\pi T_Q\left(f-\frac{n}{T_Q}\right)}+\frac{1}{2}\sum_{l,m,n}\\ &\quad\frac{1}{2}U_c\left(k_x-\frac{l}{\Delta_x},k_y-\frac{m}{\Delta_y}-\frac{1}{2\Delta_y},f-\frac{n}{T_Q}\right)e^{j\pi T_Q\left(f-\frac{n}{T_Q}\right)}\\ &=\frac{1}{2}\sum_{l,m,n} U_c\left(k_x-\frac{l}{\Delta_x},k_y-\frac{m}{2\Delta_y},f-\frac{n}{T_Q}\right)\\ &\quad\times\left(1+(-1)^{m+n}e^{j\pi T_Q f}\right).\end{aligned}\tag{5}$$

By comparing (1) with (5), one can see that although $U(k_x,k_y,f)$ is obtained by the periodic repetition of $U_c(k_x,k_y,f)$ on the points of lattice

$$\left\{\frac{l}{\Delta_x},\frac{m}{2\Delta_y},\frac{n}{T_Q},l,m,n\in Z,(m-n)=0 \bmod 2\right\}\tag{6}$$

$\bar{U}(k_x,k_y,f)$ is obtained by the periodic repetition of $U_c(k_x,k_y,f)$ on the points of lattice

$$\left\{\frac{l}{\Delta_x},\frac{m}{2\Delta_y},\frac{n}{T_Q},l,m,n\in Z\right\}\tag{7}$$

weighted by function $\left[\left(1+(-1)^{m+n}e^{j\pi fT_Q}\right)/2\right]$.

It is worth noticing that since $e^{j\pi fT_Q}$ is periodic with period equal to $2/T_Q$, expression (5) is periodic along f with period equal to $1/T_Q$. This is consistent with the fact that $\bar{u}(l\Delta_x,m\Delta_y,nT_Q)$ is sampled along the temporal axis with sampling period equal to T_Q.

The expression of $U_n(k_x,k_y)$ can be obtained by using the integration property of the Fourier transform on (3), namely

$$U_n(k_x,k_y)=\int_0^{1/T_Q} e^{j2\pi nT_Qf}\,\bar{U}(k_x,k_y,f)\,df.\tag{8}$$

For the sake of simplicity, in the following, we will refer to the first composite frame of the sequence, i.e., to $n=0$.

B. The Global Translation Case

Consider a case of global translation, in which each point of the focal plane image moves with velocity $\boldsymbol{v}=\left(v_x=\frac{s_x}{T_F},v_y=\frac{s_y}{T_F}\right)^T$, i.e.

$$u_c(x,y,t)=u_s(x-v_xt,y-v_yt).\tag{9}$$

As is well known, the relationship between the Fourier transforms $U_c(k_x,k_y,f)$ of $u_c(x,y,t)$ and $U_s(k_x,k_y)$ of $u_s(x,y)$ is

$$U_c(k_x,k_y,f)=U_s(k_x,k_y)\delta(f+v_xk_x+v_yk_y).\tag{10}$$

By substituting (10) into (5), from (8), one has

$$\begin{aligned}U_0(k_x,k_y) &=\frac{1}{2}\int_0^{1/T_Q}\sum_{l,m,n=-\infty}^{\infty} U_s\left(k_x-\frac{l}{\Delta_x},k_y-\frac{m}{2\Delta_y}\right)\\ &\quad\cdot\delta\left(f-\frac{n}{T_Q}+v_x\left(k_x-\frac{l}{\Delta_x}\right)+v_y\left(k_y-\frac{m}{2\Delta_y}\right)\right)\\ &\quad\times\left(1+(-1)^{m+n}e^{j\pi fT_Q}\right)df\\ &=\sum_{l,m=-\infty}^{\infty} e^{-j\pi\left(s_x\left(k_x-\frac{l}{\Delta_x}\right)+s_y\left(k_y-\frac{m}{\Delta_y}\right)\right)}\\ &\quad\times U_s\left(k_x-\frac{l}{\Delta_x},k_y-\frac{m}{\Delta_y}\right)\\ &\quad\times\cos\left(\pi\left(s_x\left(k_x-\frac{l}{\Delta_x}\right)+s_y\left(k_y-\frac{m}{\Delta_y}\right)\right)\right)\\ &\quad+je^{j\pi\frac{s_y}{2\Delta_y}}U_s\left(k_x-\frac{l}{\Delta_x},k_y-\frac{1}{2\Delta_y}-\frac{m}{\Delta_y}\right)\\ &\quad\times\sin\left(\pi\left(s_x\left(k_x-\frac{l}{\Delta_x}\right)+s_y\left(k_y-\frac{1}{2\Delta_y}-\frac{m}{\Delta_y}\right)\right)\right).\end{aligned}\tag{11}$$

In order to appreciate global translation effects on the spectrum of the composite frame, assume $u_s(x,y)$ is bandlimited within an elementary cell $\mathcal{V}$ [3] of lattice $\{l/\Delta_x,m/2\Delta_y\}$, i.e..

$$U_s(k_x,k_y)=0,\quad (k_x,k_y)\notin\mathcal{V}\tag{12}$$

In a suitable elementary cell $\mathcal{P}$ of lattice $\{l/\Delta_x,m/\Delta_y,l,m\in Z\}$ |3|, the power density spectrum of $u_0(x,y)$ under condition (12) is

$$\begin{aligned}|U_0(k_x,k_y)|^2 &=|U_s(k_x,k_y)|^2\cos^2\left(\pi(s_xk_x+s_yk_y)\right)\\ &\quad+\left|U_s\left(k_x,k_y-\frac{1}{2\Delta_y}\right)\right|^2\\ &\quad\times\sin^2\left(\pi\left(s_xk_x+s_y\left(k_y-\frac{1}{2\Delta y}\right)\right)\right).\end{aligned}\tag{13}$$

The above expression is interesting in that it shows that spectrum $|U_0(k_x,k_y)|^2$ (within the elementary cell $\mathcal{P}$) is the sum of two terms supported by disjoint sets: One is the "low-pass"component $|U_s(k_x,k_y)|^2$ weighted by function $\cos^2(\pi(s_xk_x+s_yk_y))$, and the other one is the "high-pass" component formed by the (frequency domain) shifted version of $[|U_s(k_x,k_y)|^2\sin^2(\pi(s_xk_x+s_yk_y))]$.

C. An Example: A Moving Grating

It may be instructive to consider (11) in the specific case of a signal $u_s(x,y)$ with a simple spectrum, such as a grating (spatial sinusoid) of spatial period $\boldsymbol{P}=(P_x,P_y)^T$

$$\begin{aligned}u_s(x,y)&=\sin\left(2\pi\left(\frac{x}{P_x}+\frac{y}{P_y}\right)\right),\\ &\quad 0\le P_x<\frac{\Delta_x}{2},\quad 0\le P_y<\frac{\Delta_y}{4}.\end{aligned}\tag{14}$$

The Fourier transform of $u_s(x,y)$ is simply

$$\begin{aligned}U_s(k_x,k_y)&=\left(\delta\left(k_x+\frac{1}{P_x},k_y+\frac{1}{P_y}\right)\right.\\ &\quad\left.-\delta\left(k_x-\frac{1}{P_x},k_y-\frac{1}{P_y}\right)\right)\Big/2j.\end{aligned}\tag{15}$$

Equation (11) shows that the composite frame $u_0(l\Delta_x,m\Delta_y)$ of the moving grating coincides with the following continuous signal:

$$\begin{aligned}u_d(x,y)&=\sin\left(2\pi\left(\frac{x-\frac{s_x}{2}}{P_x}+\frac{y-\frac{s_y}{2}}{P_y}\right)\right)\cos\left(\pi\left(\frac{s_x}{P_x}+\frac{s_y}{P_y}\right)\right)\\ &\quad-\cos\left(2\pi\left(\frac{x-\frac{s_x}{2}}{P_x}+\left(y-\frac{s_y}{2}\right)\left(\frac{1}{P_y}-\frac{1}{2\Delta_y}\right)\right)\right)\\ &\quad\times\sin\left(\pi\left(\frac{s_x}{P_x}+\frac{s_y}{P_y}\right)\right)\end{aligned}\tag{16}$$

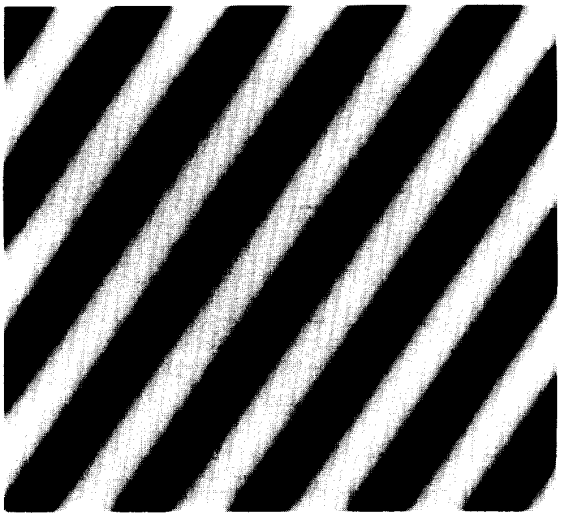

Fig. 1. Spatial grating with $\boldsymbol{P} = (P_x = 50 \text{ pels}, P_y = 80 \text{ pels})^T$.

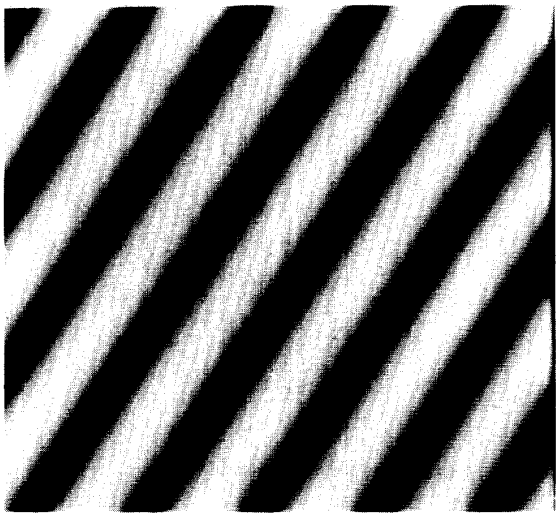

Fig. 2. Composite frame of the spatial grating of Fig. 1 moving with $\boldsymbol{v} = (v_x = 8 \text{ pels}/T_F, v_y = 0 \text{ pels}/T_F)^T$ (interlace ratio 2:1).

sampled on lattice

$$\Gamma = \{l\Delta_x, m\Delta_y, l, m \in Z\}. \tag{17}$$

Signal $u_d(x, y)$ is the sum of a pair of spatial sinusoids respectively weighted by constants $[\cos(\pi(\frac{s_x}{P_x} + \frac{s_y}{P_y}))]$ and $[\sin(\pi(\frac{s_x}{P_x} + \frac{s_y}{P_y}))]$ sampled on lattice Γ.

The difference between $u_d(x, y)$ and $u_s(x, y)$ explains the visual effects of the composite frames of gratings. One example of the visual effect of a global translation by vector $\boldsymbol{s} = (s_x = 8 \text{ pels}/T_F, s_y = 0 \text{ pels}/T_F)^T$ of the spatial sinusoid of period $\boldsymbol{P} = (P_x = 50 \text{ pels}, P_y = 50 \text{ pels})^T$ of Fig. 1 is shown by the composite frame of Fig. 2. It is worth noting that the difference between (11) and (16) manifests itself through a diffuse blurring.

Figs. 3 and 4, respectively, show the spectrum of the sinusoid of Fig. 1 (see (14)) and of the composite frame of Fig. 2 (see (16)) in an elementary cell of dual lattice [3] Γ^*. The spectral low- and high-pass

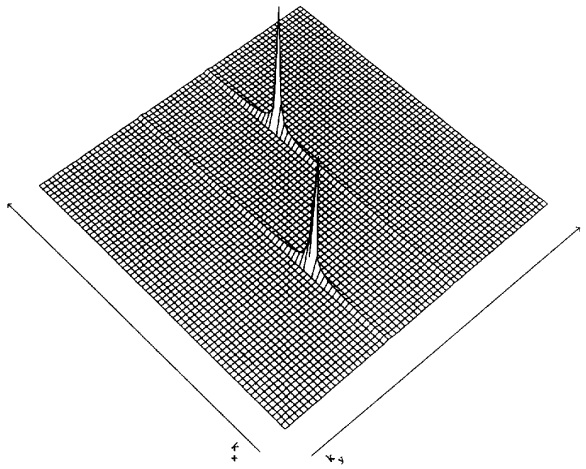

Fig. 3. Power spectrum of the grating of Fig. 1.

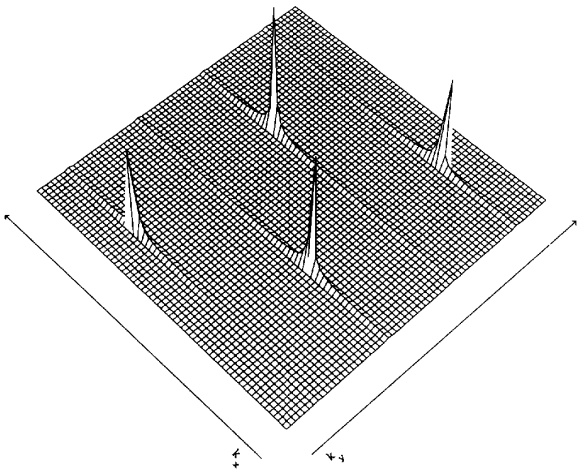

Fig. 4. Power spectrum of the composite frame of Fig. 2.

components, which are typical of the Fourier transform of composite frames, are clearly visible in Fig. 4.

The spectral characteristics noted in the simple case of the composite frame of a moving grating can be also recognized in the case of real-life imagery. Fig. 5 shows the thermogram of an object typically used to measure the modulation transfer function (MTF) of thermocameras [6]. Fig. 6 shows the thermogram of the moving object of Fig. 5 taken by a 2:1 interlaced thermocamera. The characteristic blurring previously noted is also present in Fig. 6. The power spectrum of the thermograms of Fig. 5 and Fig. 6, in an elementary cell of Γ^*, can be seen from Figs. 7 and 8, respectively. Fig. 8 clearly shows the two spectral components expected from (11).

The separation of the spectrum into two components and the high-frequency content of the blurred edges could suggest that the visual quality of the composite frame would be improved by linear smoothing. However, such an approach is not very effective. One reason for this is that if $u_s(x, y)$, for instance, is vertically bandlimited, as is (12), then the output of a filter with a passband equal to the spectral support of $u_s(x, y)$ is the sampled version of $[(u_s(x, y) + u_s(x - s_x, y - s_y))/2]$. In this case, the signal information is in a single field, and interpolating the odd

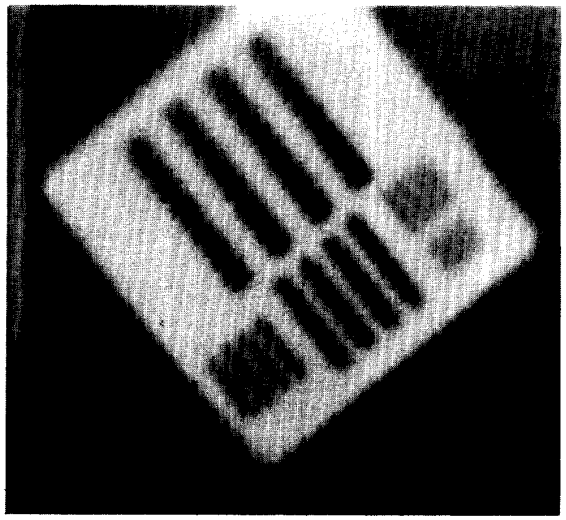

Fig. 5. Thermogram of a still object.

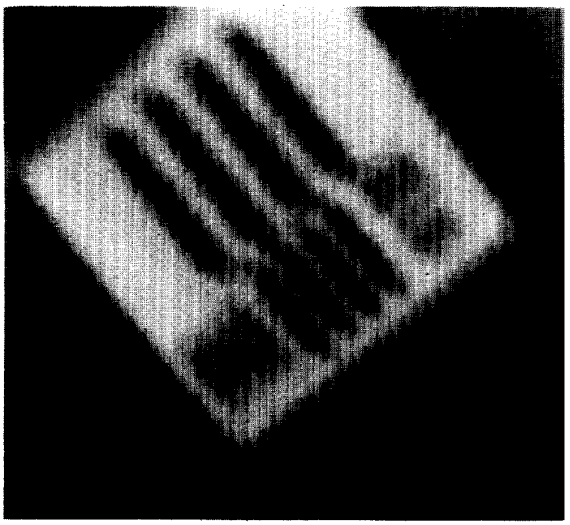

Fig. 6. Thermogram of the object of Fig. 5 moving with $\boldsymbol{v} = (v_x = 8 \text{ pels}/T_F, v_y = 5, \text{ pels}/T_F)^T$ (interlace ratio 2:1).

lines from the even lines (or vice-versa) would be a better way of restoring the composite frame. In most practical cases, however, the band-limitation assumption is not verified, and this simple recovery procedure is not applicable. The technique described in Section III is able to handle such general situations.

III. Motion-Compensated Restoration of Composite Frames

As exemplified by Figs. 2 and 6, the composite frames of moving objects are likely to lose object definition and eventually intelligibility, expecially in highly textured images. The frequency domain analysis results of the previous section may be profitably used in order to devise a simple algorithm for "deblurring" composite frames from motion induced artifacts. A key problem for the proposed method is how to determine displacement vector $\boldsymbol{s}$ from a single composite frame.

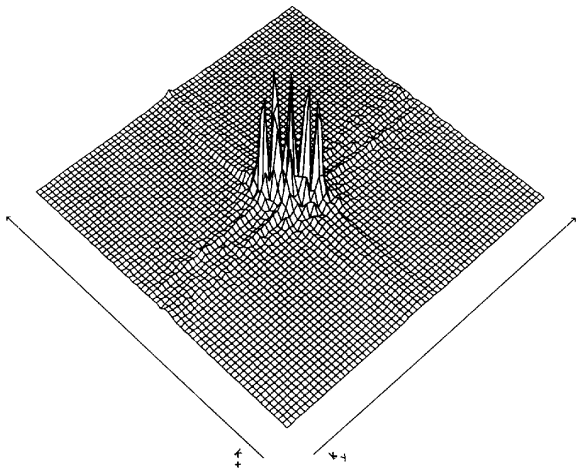

Fig. 7. Power spectrum of the thermogram of Fig. 5.

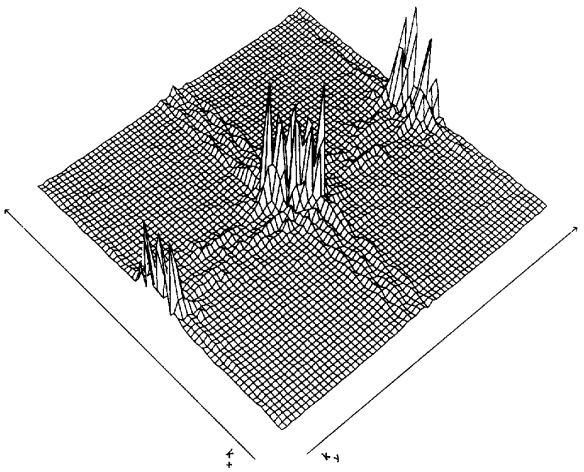

Fig. 8. Power spectrum of the thermogram of Fig. 6.

Motion detection algorithms typically use several frames exclusively, utilizing even (or odd) lines fields when dealing with signals obtained from interlaced scanning. As the displacement detection technique presented in this work shows, the same information can be obtained by means of the even and odd fields of a single frame. Its operation is reminiscent of a well-known correlation-based algorithm called *phase correlation* [7]–[10]. In contrast to the original method, the technique of this work exploits the possibility (suggested by the frequency domain results of Section II) of displacement estimation derived from the two interlaced fields of a single frame.

Once the displacement vector $\boldsymbol{s}$ has been found, the restoration is carried out by simply shifting the second field of vector $\boldsymbol{s}$. If an approximation of $\boldsymbol{s}$ belonging to lattice $\{l\Delta_x, 2m\Delta_y, l, m \in Z\}$ is used as the shift vector, no interpolation is necessary.

Consider (11) under the band-limiting hypothesis (12), and assume that image displacement during period T_F is

$$\boldsymbol{s} = (s_x, s_y)^T = (l_0\Delta_x, 2m_0\Delta_y)^T, \quad l_0, m_0 \in Z. \tag{18}$$

Within a suitable elementary cell $\mathcal{P}$ of lattice Γ (17), the following

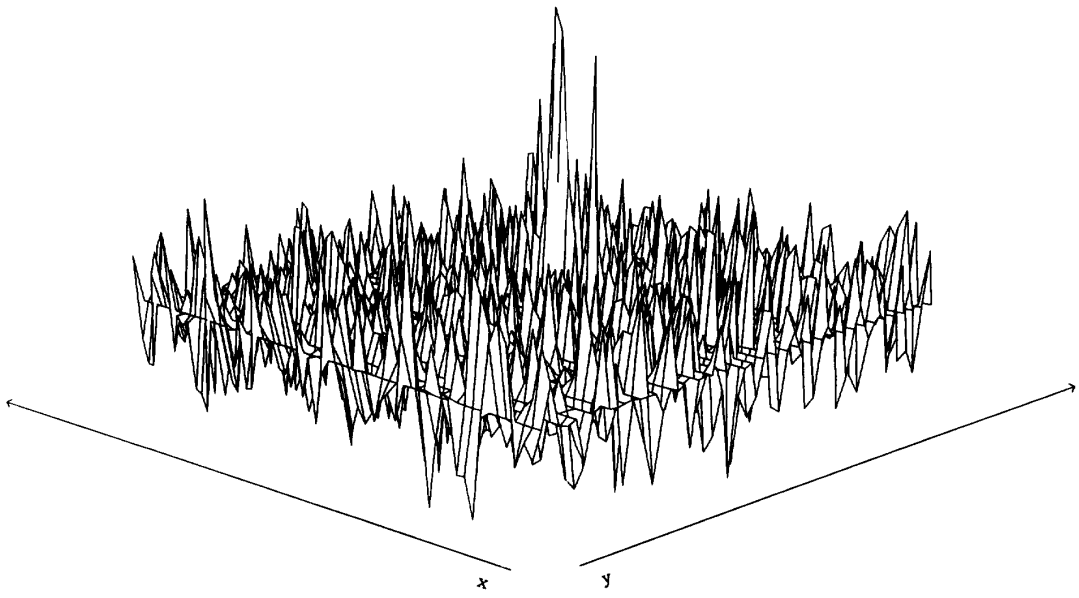

Fig. 9. Spatial function (21) relative to the thermogram of Fig. 6.

relationships hold:

$$U_0(k_x, k_y) + U_0\left(k_x, k_y + \frac{1}{2\Delta_y}\right) = U_s(k_x, k_y) + U_s\left(k_x, k_y + \frac{1}{2\Delta_y}\right) \tag{19}$$

$$U_0(k_x, k_y) - U_0\left(k_x, k_y + \frac{1}{2\Delta_y}\right) = e^{-j2\pi(s_x k_x + s_y k_y)}\left(U_s(k_x, k_y) + U_s\left(k_x, k_y + \frac{1}{2\Delta_y}\right)\right). \tag{20}$$

Hence, we have

$$\mathcal{F}^{-1}\left[\frac{U_0(k_x, k_y) - U_0\left(k_x, k_y + \frac{1}{2\Delta_y}\right)}{U_0(k_x, k_y) + U_0\left(k_x, k_y + \frac{1}{2\Delta_y}\right)}\right] = \delta((l - l_0)\Delta_x, (m - 2m_0)\Delta_y) \tag{21}$$

where $\mathcal{F}^{-1}$ denotes the inverse Fourier transform operator, and $\delta(\cdot, \cdot)$ is the 2-D discrete impulse. The components of $\boldsymbol{s}$ can be clearly determined by localizing the maximum of function (21). For practical implementation purposes, expression (21) can be computed by means of 2-D FFT algorithms [7], whose computational efficiency is well known.

The method can also be put to work in the case of nonbandlimited signals by performing a suitable regularization of the input. In fact, if the input signal is forced to be bandlimited by an appropriate low-pass filtering, the deblurring will still be correct. A simple but effective way of implementing such a provision is given by setting a suitable set of DFT coefficients [7] equal to zero. Practical tests with real-world composite frames have shown that forcing to zero half, or three quarters, of the DFT coefficients gives sufficiently accurate results.

In the case of thermographic images, however, it should be noted that the typical low-pass characteristics of the modulation transfer function [6] of thermocameras make for well band-limited input signals.

Fig. 9 shows a 64× 64 plot of spatial function (21) relative to the thermogram of Fig. 6. The position of the maximum of Fig. 9 coincides with the true image displacement associated with velocity $\boldsymbol{v} = (8 \text{ pels}/T_F, 5 \text{ pels}/T_F)^T$. (For a treatment of the robustness of the phase-correlation algorithm with respect to noise and to scene characteristics, see [7]–[11].)

ACKNOWLEDGMENT

Dr. E. Grinzato of CNR-ITEF of Padova is acknowledged for kindly supplying the thermographic material used in our experimentation.

REFERENCES

[1] W. K. Pratt, *Digital Image Processing*. New York: Wiley, 1978.
[2] Z. K. Liu and J. Y. Xiao, "Restoration of blurred tv pictures caused by uniform linear motion," *Comput. Vision, Graphics, Image Processing*, vol. 44, pp. 30–34, 1988.
[3] E. Dubois, "The sampling and reconstruction of time-varying imagery with applications in video systems," *Proc. IEEE*, vol. 73, pp. 502–522, Apr. 1985.
[4] R. A. F. Belfor, R. L. Lagendijk, and J. Biemond, "Subsampling of digital image sequences using motion information," in *Motion Analysis and Image Sequence Processing* (M. I. Sezan and R. L. Lagendijk, Eds.). Boston: Kluwer, 1993.
[5] B. Girod and R. Thoma, "Motion compensated field interpolation for interlaced and noninterlaced grids," in *Proc. SPIE Conf. Image Coding*, 1985, pp. 186–193, vol. 594.
[6] S. K. Parks, R. Schowengerdt, and M. Kaczynski, "Modulation-transfer-function analysis for sampled image systems," *Applied Opt.*, vol. 23, no. 15, pp. 2572–2582, Aug. 1984.
[7] J. J. Pearson, D. C. Hines, S. Golosman, and C. D. Kuglin, "Video rate image correlation processor," in *Proc. SPIE (IOCC 1977)*, pp. 197–204.
[8] C. D. Kuglin, A. F. Blumenthal, and J. J. Pearson, "Map-matching techniques for terminal guidance using Fourier phase information," in *Proc. SPIE—Digital Processing Aerial Images*, 1977, pp. 21–29, vol. 186.
[9] G. A. Thomas and B. A. Hons, "Television motion measurements for DATV and other applications," BBC Tech. Rep., RD 1987/11.
[10] S. Alliney and C. Morandi, "Digital image registration using projections," *IEEE Trans. Patt. Anal. Machine Intell.*, vol. PAMI-8, no. 2, pp. 222–233, Mar. 1986.
[11] R. Manduchi and G. A. Mian, "Accuracy analysis for correlation-based image registration algorithms," in *Proc. IEEE ISCAS'93*, 1993, pp. 834–837, vol. 1.